International Journal of Pharmaceutics 434 (2012) 183–190

Contents lists available at SciVerse ScienceDirect

International Journal of Pharmaceutics

journal homepage: www.elsevier.com/locate/ijpharm

Study of the potential of stratum corneum lipids and exogenous molecules interaction by fluorescence spectroscopy for the estimation of percutaneous penetration

Elsa Jungman*, Cécile Laugel, Athéna Kasselouri, Arlette Baillet-Guffroy

Group of Analytical Chemistry Paris Sud (EA 4041), Faculty of Pharmacy, Université Paris-Sud, 5 rue Jean-Baptiste Clément, 92290 Chatenay-Malabry, France

ARTICLE INFO

Article history:
Received 26 March 2012
Received in revised form 22 May 2012
Accepted 22 May 2012
Available online 30 May 2012

Keywords:
Percutaneous absorption
Ceramides
Fluorescence spectroscopy
Predictive model

ABSTRACT

Considering that the skin barrier properties are closely linked to the ceramides composition and conformation within the SC, our work focused on developing a new evaluation criterion in complement of the Log Pow and MW: lipids retentive role within the SC. We developed an in vitro model to study exogenous molecules (Mol) and SC lipids interaction by fluorescence spectroscopy. As ceramides do not fluoresce, fluorescence probes that emit a fluorescence signal in contact with lipidic chains were selected for the study. A protocol was developed based on the exogenous molecule (cosmetic actives) affinity for the SC lipids. A fluorescence criterion (ΔI) was calculated from our results and compared to ex vivo skin penetration measurements realized with a Franz cell device. Our results indicated that polarity seems to be very representative of the ceramide and exogenous molecule interaction for most of the molecules tested. However, the ΔI calculated highlighted the particular interaction of some exogenous molecules with ceramides and their skin distribution. This particular behavior was not initially possible to estimate with the Log Pow and MW. This work aimed to develop a new alternative method to enhance the percutaneous penetration estimation of exogenous molecules for the risk analysis.

1. Introduction

The main function of the skin is to protect the human body against water loss, ultraviolet light and chemical absorption. The stratum corneum (SC), the outermost epidermal layer, plays a central role to achieve this function. It is composed of dead cells, corneocytes, embedded in a unique lipidic matrix. The SC lipidic matrix is mainly composed of ceramides, cholesterol and long-chain free fatty acids (Kessner et al., 2008). The lipid composition and organization is essential to maintain the cutaneous barrier function (Joo et al., 2010). Ceramides are known to play a key role in structuring the SC, they consist of a sphingoid base N-acylated by a long chain of fatty acid. Recently, eleven classes of CER have been determined (Masukawa et al., 2008). Their structural variety results from possible combination between 4 types of sphingoid base (sphingosine, phytosphingosine, 6-hydroxysphingosine or dihydrosphingosine) and 3 types fatty acids (non-hydroxyacids, α or ω hydroxyacids) (Kessner et al., 2008; Wartewig and Neubert, 2007). The acyl chain length is variable from 18 to 32 carbons. The long hydrophobic ceramides chains are essential to maintain the barrier properties. Short chains ceramides are able to increase significantly skin permeability to drugs (Novotný et al., 2009; Janůšová et al., 2011). Also a change in their composition can be associated with a change in the lamellar lipid organization in atopic eczema patients that altered then their SC properties (Janssens et al., 2011).

With the banned of animal testing in the cosmetic industries, there is a need to develop efficient alternative methods to predict the percutaneous penetration of cosmetics ingredients. Many in vitro and in vivo methods are referred to study the absorption of chemicals through the skin (Benson and Watkinson, 2011). Without in vivo methods validated yet the current in vitro guidelines for percutaneous penetrations are referenced by the OECD and SCCS (OECD, 2008; SCCS, 2010). The issue with in vitro tests is their limitations due to the lack of homogeneity between the experiments i.e. skin type (animals or human) or skin treatment (full thickness or dermatomed). In a recent draft, the OECD recommended (OECD, 2010) that the prediction of percutaneous penetration should be based on structural characteristics of these molecules i.e. Log Pow (polarity) and MW (molecular mass). If the MW of a molecule is

Abbreviations: SC, stratum corneum; CER, ceramide; Log Pow, partition coefficient; MW, molecular mass; K_p, permeation coefficient; Mol, exogenous molecules; DPH, 1,6-diphenyl-1,3,5-hexatriene; *m*-THPP, 5,10,15,20-tetrakis (3-hydroxyphenyl)-21H,23H-porphirine; LIP, cutaneous lipids; EA, ethyl acetate; OC, octocrylene; OS, octisalate; OX, octinoxate; BP3, benzophenone 3; BP, butyl paraben; CAF, caffeine; PRED, prednisolone; MP, methyl paraben; EP, propyl paraben; EP, epidermis; DE, dermis; TS, tape stripping; EP_{tot}, total epidermis; I_{fluo}, fluorescence intensity; LOD, limit of detection; LOQ, limit of quantification.

* Corresponding author. Tel.: +33(0)146835389; fax: +33(0)146835389.
E-mail address: elsa.jungman@gmail.com (E. Jungman).

0378-5173/$ – see front matter © 2012 Elsevier B.V. All rights reserved.
http://dx.doi.org/10.1016/j.ijpharm.2012.05.049

Table 1
Exogenous molecules studied, ranged by increasing Log Pow.

Molecules		Properties	MW	Log Pow
Caffeine	CAF	Cellulite reduction	196	−0.07
Prednisolone	PRE	Corticosteroid	360	1.62
Methyl paraben	MP	Preservative	152	1.93
Ethyl paraben	EP	Preservative	166	2.27
Propyl paraben	PP	Preservative	180	2.81
Butyl paraben	BP	Preservative	194	3.53
Benzophenone 3	BP3	UV filter	228	3.79
Octisalate	OS	UV filter	250	5.77
Octinoxate	OX	UV filter	290	5.8
Octocrylene	OC	UV filter	361	6.88

≤500 g/mol and the Log Pow is between −1 and +4, a 100% percutaneous penetration can be considered. Outside these criteria, it is considered at 10%. Studies tried to improve the OECD prediction using models including more parameters such as the vehicle and formulation (Ghafourian et al., 2010; Grégoire et al., 2009).

Many mathematical models can be found in the literature. Most of the models predict skin permeability from two parameters, Log Pow and MW i.e. Potts and Guy model (Guy and Potts, 1992).

Potts and Guy mathematical model :

$$\text{Log}\,K_p\,(\text{cm/s}) = 0.71\text{Log Pow} - 0.0061\text{MW} - 6.3$$

Lian correlated permeation results with predictive models and the best prediction found was from Mitragotri mathematical model, but with only a R^2 of 0.698 a little higher than the Potts and Guy model, $R^2 = 0.676$ (Lian et al., 2008). These empirical models fit mostly for molecules with a Log Pow comprised between 0 and 4. The Potts and Guy model cannot predict the permeation for molecules with a Log Pow above +6.

Considering that the skin barrier properties are closely linked to the lipidic composition and conformation within the SC, our work focused on developing a new evaluation criterion for the prediction of percutaneous penetration in complement of the Log Pow and MW: lipids retentive role within the SC.

We developed an in vitro model to study exogenous molecules (Mol) and SC lipids interaction by fluorescence spectroscopy. As ceramides do not fluoresce, fluorescence probes that fluoresce in contact with lipidic chains were selected for the study. The protocol was developed based on exogenous molecules (cosmetic actives) affinity for the SC lipids.

A probe in solution was first mixed with a lipidic solution (ceramides). The interaction between the probe and lipids increased the fluorescence emission of the probe. Then an exogenous molecule was added to the probe–lipid solution. If the molecule had affinity for the lipid, the molecule–lipid interaction removed the probe from the lipidic chain and decreased in consequence the fluorescence intensity (I_{fluo}).

Three equilibrium were implied:

$$[\text{Probe}] + [\text{Lipid}] \rightleftharpoons [\text{Probe–Lipid}] \quad (k_1)$$

$$[\text{Lipid}] + [\text{Mol}] \rightleftharpoons [\text{Lipid–Mol}] \quad (k_2)$$

$$[\text{Probe}] + [\text{Mol}] \rightleftharpoons [\text{Probe–Mol}] \quad (k_3)$$

To establish a simple predictive model of SC lipids and exogenous molecules interaction, our work was conducted according the following experimental design. The study included various exogenous molecules (UV filters, preservatives, corticoid and cosmetic actives) i.e. Log Pow ranging between −0.07 and 6.88 and MW between 152 and 361 g/mol (Table 1). In preliminary studies, operating conditions were set in two steps:

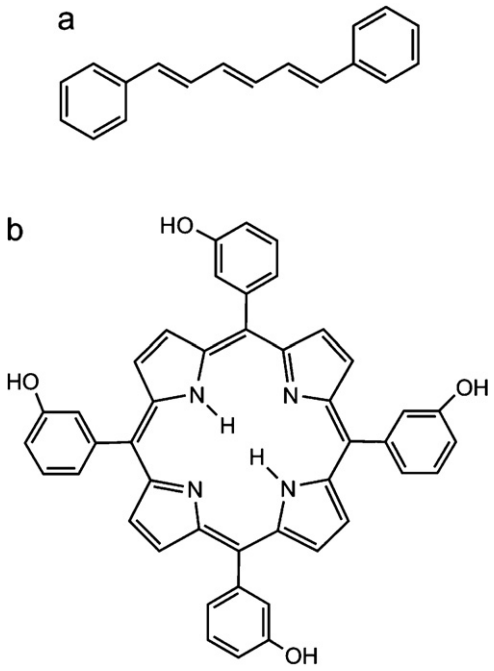

Fig. 1. The two fluorescence probes tested for the study: (a) 1,6-diphenyl-1,3,5-hexatriene (DPH) and (b) 5,10,15,20-tetrakis(3-hydroxyphenyl)-21H,23H-porphine (*m*-THPP).

first, the appropriate fluorescent probe was chosen between the 1,6-diphenyl-1,3,5-hexatriene (DPH) and 5,10,15,20-tetrakis (3-hydroxyphenyl)-21H,23H-porphirine (*m*-THPP) (Fig. 1), according to the stability of the probe–lipid complex fluorescence. These probes have no fluorescence in a polar environment but strongly fluoresced in a hydrophobic media. Previous study revealed that in contact with lipidic chains they emitted a fluorescence signal as a result of non-covalent interaction (Zhou et al., 1999; Caudron et al., 2005; Ibrahim et al., 2011). In a second step, different synthetic ceramides (Fig. 2) (saturated: Ceramide 2 (Cer 2) or unsaturated: Ceramide IIIa (Cer IIIa)) and SC lipids extracted from human skin were tested with a constant probe concentration and various molecules concentration. A lipid was selected according to the intensity and the stability of the [probe–lipid] fluorescence.

The second part of our study was to develop the predictive approach. We tested the selected lipid with the molecules at a constant concentration and the probe at various concentrations. A SC lipids and exogenous molecule interaction fluorescence criterion, ΔI, was calculated from our results. ΔI was validated by

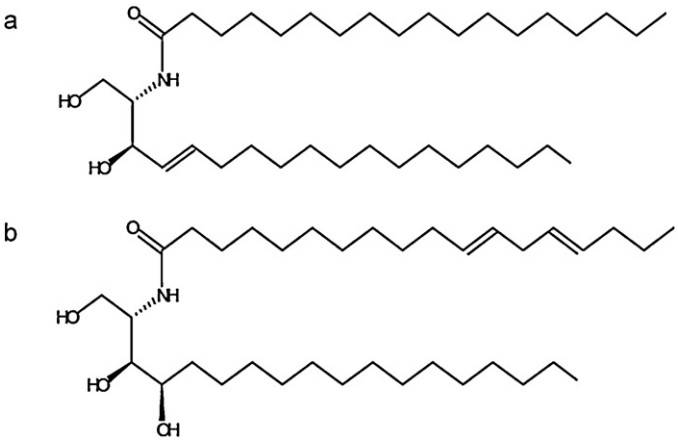

Fig. 2. Synthetic lipids tested. (a) Ceramide 2 (Cer 2) and (b) Ceramide IIIa (Cer IIIa).

comparing its values with ex vivo skin penetration measurements realized with a Franz cell device coupled to HPLC analysis. This work aimed to develop a new alternative method to enhance the percutaneous penetration estimation of exogenous molecules for the risk analysis.

2. Materials and methods

2.1. Chemicals and materials

Exogenous molecules: benzophenone 3, methyl, ethyl, propyl and butyl parabens, octinoxate and octisalate were purchased at Sigma–Aldrich (Saint-Quentin Fallavier, France). Octocrylene (Parsol 40®) at DSM (Courbevoie, France). Caffeine was purchased at Alfa Aesar (Schiltigheim, France) and the prednisolone at Molekula (Dorset, United-Kingdom).

Synthetic ceramides: Cer 2 was purchased at Sederma (Le Perray, France) and Cer IIIa at Evonik Industries (Essen, Germany).

Stratum corneum lipids (LIP) extraction: Squares of 3 cm × 3 cm were designed on skin surface from abdominal biopsies of human volunteers. Four cotton swabs drenched in a mixture of EA/MeOH (20:80, v/v) were used for each square. Each cotton swab was rubbed 10 times on each square and plunged into 2 ml of a mixture of chloroform/methanol ($CHCl_3$/MeOH) (2:1, v/v) during a few minutes. After removing the cotton swabs, solutions were centrifuged at 4000 rpm for 10 min to eliminate some cotton particles and skin cells elements. The homogeneous phase containing the lipids was recuperated and evaporated. Residues were recuperated in MeOH and diluted at a concentration of 2×10^{-5} M approximately; calculated from an average lipid molecular mass of 400 g/mol.

Fluorescent probes: DPH was purchased at Sigma–Aldrich (Saint-Quentin Fallavier, France) and the *m*-THPP at Frontier Scientific (Logan, UT, USA).

Bovine serum albumin was purchased at Sigma–Aldrich (Saint-Quentin Fallavier, France). Sodium chloride salts was purchased at Carlo Erba Réactifs-Sds (Val de Reuil, France).

HPLC grade methanol was purchased at Sigma–Aldrich (Saint-Quentin Fallavier, France). Acetic acid was purchased at Prolabo (VWR, Fontenay Sous Bois, Bois).

Fluorescence measurements were performed with a spectrofluorimeter equipped with a red sensitive photomultiplier (Perkin-Elmer, LS50B, Courtaboeuf, France). Excitation and emission wavelengths were set at 419 and 648 nm, respectively, for *m*-THPP and at 357 and 428 nm for DPH. Data acquisition was performed with FL WinLab Software (Perkin-Elmer, Courtaboeuf, France).

The HPLC was composed of an autosampler (HPLC 565 Autosampler), a column thermostat (HPLC 582 column thermostast), a diode array detector (HPLC 545V diode array detector), a pump (System 525) and a degasser (3493 Degasser). All these elements were purchased at Kontron (Toulon, France). Two C18 columns (150 mm × 4.6 mm and 250 mm × 4.6 mm, Kromasil, AIT, Houilles, France) and C18 guard columns (Kromasil C18, 5 mm Guard Column Cartridges, Supelco, Bellefonte, PA, USA) were used. Mobile phase composition was improved for each exogenous molecule to achieve a good selectivity from skin endogenous compounds. Data acquisition was performed with Kroma system 2000 software (Kontron Instruments, Italy). A specific detection wavelength was set for each molecule using a Cary Bio 300 spectro-photometer (Varian, USA).

2.2. Preparation of the solutions

2.2.1. Fluorescence spectroscopy

Ceramides: Methanolic solutions of lipids (Cer 2 and Cer IIIa) were conserved at a concentration of 10^{-4} M. Stock solutions were diluted in series in methanol (MeOH) to reach 2×10^{-5} M. Lipids solutions (Cer 2, Cer IIIa and LIP) were conserved at −20 °C.

Probes: Stock solutions of DPH and *m*-THPP were prepared respectively in MeOH at 4×10^{-4} M and 7×10^{-5} M. These stock solutions were diluted in series daily at a concentration of 2×10^{-7} M in Millipore Q water. All solutions were hidden from light and conserved at −20 °C.

Exogenous molecules were diluted in MeOH at 10^{-2} M, 10^{-4} M and 10^{-5} M and conserved at −20 °C before use.

2.2.2. Percutaneous penetration

Exogenous molecules were diluted in ethyl acetate (EA) at 10^{-2} M and conserved at −20 °C before use.

2.3. Protocols

2.3.1. Fluorescence spectroscopy

2.3.1.1. Preliminary study. Choice of the probe: First, a methanolic solution of Cer 2 at 2×10^{-5} M was mixed with an aqueous solution of DPH or *m*-THPP at 2×10^{-7} M with a ratio of 85/15 (v/v). Fluorescence intensity was then recorded during 60 min. Then, the stability of lipids solution (Cer 2, Cer IIIa and LIP) at 2×10^{-5} M mixed with DPH at 2×10^{-7} M was followed during 60 min by fluorescence. At last, the variation of fluorescence intensity with the DPH probe was recorded with variable Cer 2 concentrations ranging from 10^{-6} M to 10^{-4} M.

Choice of the lipidic model and experimental parameters: An aqueous DPH solution at 2×10^{-7} M was mixed with a 2×10^{-5} M methanolic lipid (Cer 2, Cer IIIa or LIP) solution with a ratio of 85/15 (v/v) respectively. The molecule of interest was added at different increasing concentrations to the [probe–lipid] solution, ranging from 5×10^{-7} M to 4×10^{-5} M final concentration. A DPH–MeOH (85/15) (v/v) solution was used as a blank. After 10 min, the fluorescence was measured for each molecule concentration. In parallel, to check any background noise, the same molecules of interest concentration were added directly to the 2×10^{-7} M DPH aqueous solution without lipids. Experiments were realized in triplicate.

2.3.1.2. Predictive approach: determination of the [Cer IIIa–Molecule] interaction criterion. Variation of the probe concentration: First, DPH was diluted into water at a concentration ranging from 10^{-9} to 2×10^{-6} M. The aqueous DPH solution was mixed with Cer IIIa at 2×10^{-5} M in methanol with a ratio of 85/15 (v/v) respectively. The molecule of interest was added at a 10^{-5} M final concentration to the DPH–Cer IIIa solution. The fluorescence was measured 10 min after the addition of the molecule. In parallel, an appropriate DPH solution without lipids was prepared, the ratio 85/15 (v/v) was kept with pure methanol instead of a lipid methanolic solution. Its fluorescence intensity was systematically subtracted from the fluorescence intensity of the probed lipid solution with and without the addition of the exogenous molecule.

2.3.2. Percutaneous penetration studies

2.3.2.1. Preparation of the human skin and Franz cells. Fat was removed from fresh skin from abdominal plastic surgery. Skin was stored at −25 °C and full thickness skin was used for the experiments. Before the experiment the skin was immersed in physiologic serum (0.85% NaCl) for 20 min and then cut in circle shapes to fit the glass diffusion cells. Each skin was carefully washed with Millipore Q water and dried with paper before to be mounted on the Franz cell. Franz cells had a diameter of 2 cm^2 and a volume of liquid receptor of 11.5 ml (Lara Spirals, Couternon, France). A magnetic stirrer bar was added in the donor compartment. The liquid receptor was filled with distilled water containing 0.85% NaCl and 0.01% of bovine serum albumin. Air bubbles in the donor compartment were removed. The system was thermostated at 37 °C above

Table 2
Schedule of operating conditions for chromatographic analyses with methanol (MeOH), acetic acid (AA) and water (H_2O). LOD represents the limit of detection and LOQ the limit of quantification.

Molecule		Wavelength (nm)	Column	Mobile phase	Linearity (R^2)	Accuracy (%)	Repetability (%)	LOD (μM)	LOQ (μM)
Butyl paraben	BP	254	C18, 5 mm; 150 mm × 4.6 mm	50% H_2O (1% AA)/69% MeOH	0.99	5	1.1	0.45	1.5
Benzophenone 3	BP3	291	C18, 5 mm; 150 mm × 4.6 mm	31% H_2O (1% AA)/69% MeOH	0.99	3.6	0.1	0.02	0.05
Octisalate	OS	250	C18, 5 mm; 150 mm × 4.6 mm	5% H_2O (1% AA)/95% MeOH	0.99	2.8	2.4	0.78	2.6
Octinoxate	OX	290	C18, 5 mm; 150 mm × 4.6 mm	5% H_2O (1% AA)/95% MeOH	0.99	2.6	1.2	0.38	1.3
Octocrylene	OC	307	C18, 5 mm; 150 mm × 4.6 mm	21% H_2O (1% AA)/79% MeOH	0.98	7.5	0.1	0.01	0.05

a magnetic stirrer to ensure the homogeneity of the liquid receptor during the experiment. After 30 min of stabilization, 200 μl of a solution containing one of the exogenous molecules diluted in EA at 10^{-2} M was dropped on the skin surface. During the experiment Franz cells were not occluded left at open air.

2.3.2.2. Preparation of collected samples. After 22 h, the liquid receptor and the skin were collected. The skin surface was washed with a cotton swab on which 200 μl of liquid receptor (distilled water containing 0.85% NaCl and 0.01% of bovine serum albumin) was dropped. After washing, the skin surface was tape-stripped 3 times with D-squame tape (Cuderm, Dallas, USA) at the same constant pressure. The 3 tapes were pooled in a 20 ml vial and stored at −20 °C until analysis. The liquid receptor was filtrated and stored at −20 °C until analysis. The epidermis was separated from the dermis by heating and then cut into small pieces with a scalpel. The epidermis and the dermis were stored at −20 °C until analysis. The exogenous molecule was extracted from the tapes by adding 2 ml of toluene in the vial over night. The next day, tapes were removed from the vial and 1 ml of the solution recovered was diluted in methanol and filtrated (sterile filters, 0.22 μm, Roth, Lauterbourg, France) until the solution was completely limpid. The dermis and epidermis were grounded with an adapted mixer and tubes (ULTRA-TURRAX® Tube Drive and BMT-20-S tubes, IKA, Staufen, Germany) in 5 ml of methanol. The methanolic recuperated was filtrated. All solutions from collected samples were stored at −20 °C until analysis.

2.3.2.3. HPLC analysis. All samples (tapes, epidermis, dermis and liquid receptor) were quantified by HPLC analysis coupled to a UV detector. A sample of 20 μl was injected. For each analysis, standard samples were prepared ranging from 10^{-6} M to 10^{-4} M. The mobile phase and the UV wavelength used for the experiments are summarized in Table 2.

3. Results and discussion

3.1. Preliminary study

3.1.1. Probe choice

The probe was chosen regarding the fluorescence intensity and the stability of the complex [probe–lipid]. Experiments were conducted to choose the most appropriate fluorescent probe between DPH and *m*-THPP for the predictive approach. In a previous work, DPH and *m*-THPP showed high fluorescence intensity when associated to organized lipidic edifices such as micelles. *m*-THPP was shown to induce a higher response than DPH for lipids (Ibrahim et al., 2011). The interest of *m*-THPP in comparison to the other probes used for lipid detection is, from a spectroscopic point of view, to present an emission at 600–800 nm (maximum around 650 nm) and so potentially a better selectivity. Ibrahim determined the most appropriate probe–lipid ratio for the fluorescence lipidic detection at 85/15 water/methanol mixture (v/v) with either DPH or *m*-THPP. It was found that 15% of methanol (v/v) avoided precipitation of phospholipids species and resulted in the maximum difference in fluorescence emission in the presence and in the absence of lipids (Ibrahim et al., 2011). The same ratio was selected for our protocol.

In our experiments, [*m*-THPP–Cer 2] fluorescence intensity was higher than [DPH–Cer 2] after 10 min of contact. It reaches 350 AUF compared to 150 AUF for the DPH. We noticed that [*m*-THPP–Cer 2] fluorescence decreased continually during the 60 min of observation. After 60 min, *m*-THPP lost 100 AUF whereas [DPH–Cer 2] fluorescence increased during the 10 first minutes of the measurement and then staid stable during the observation.

DPH was then considered the most appropriate probe for our study due to a more stable association with the ceramide carbonyl chains. This stability is a key point to determine the interaction between ceramides and exogenous molecules without being trouble by the variation of fluorescence intensity of the complex [probe–lipid].

3.1.2. Choice of the lipidic model and experimental parameters

The lipidic model was chosen first according to the fluorescence intensity and stability of the complex [probe–lipid] with the 3 lipidic models (Cer 2, Cer IIIA and LIP). Second in function of I_{fluo} variation after addition of the molecule at various concentrations into the complex [probe–lipid] and the stability of the equilibrium regarding the molecule concentrations tested.

DPH was tested with the different lipid models. DPH fluorescence emission at 427 nm recorded a stable value after 10 min after mixing with Cer 2, Cer IIIa or LIP and remained stable for the next 60 min. Fluorescence intensity was around 360 UA for Cer 2, 400 for Cer IIIa and 190 for LIP.

Fluorescence intensity did not vary significantly with the three lipidic models after the addition of exogenous molecules at different concentrations into the solution [DPH–lipid] except for OC (Fig. 3). Two parameters were considered for OC: I_{fluo} decrease and the dynamic concentration range in which I_{fluo} decrease was noted. We observed two parts in the OC fluorescence curve after its addition into [DPH–lipid] solution.

(1) After the addition of the lowest OC concentration (5×10^{-7} M) into the [probe–lipid] solution, I_{fluo} immediately decreased and kept decreasing until the addition of a particular OC, named the threshold concentration. For low [OC], the fluorescence intensity decrease was related to the reaction:

$$[\text{Probe–Lipid}] + \text{Mol} \rightleftharpoons [\text{Mol–Lipid}] + \text{Probe}(k) \quad \text{with } k = \frac{k_2}{k_1}$$

(2) After this threshold concentration reached, I_{fluo} remained constant (Cer IIIa) or increased significantly (Cer 2 and LIP). The increase was not observed with [probe–Cer IIIa], probably according to a stronger interaction between Mol and Cer IIIa.

The fluorescence intensity increase (for Cer 2 and LIP) was related to the reaction:

$$[\text{Probe–Lipid}] + \text{Mol} \rightleftharpoons [\text{Probe–Mol}] + \text{Lipid} \quad (k') \text{ with } k' = \frac{k_3}{k_1}$$

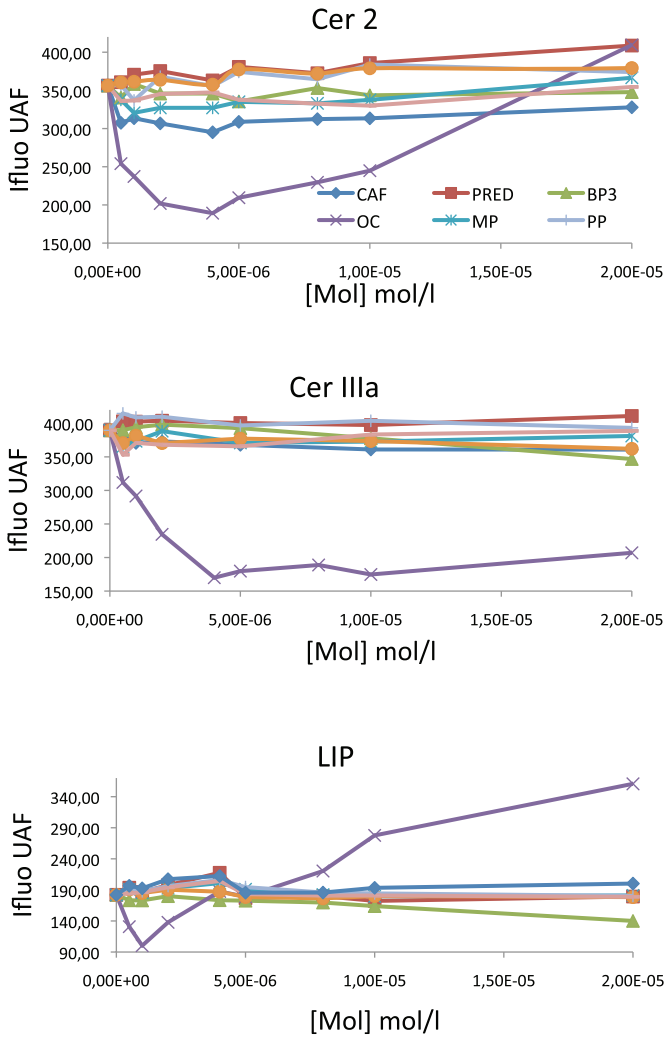

Fig. 3. Fluorescence curves obtained with a constant DPH concentration and each of the three lipidic models tested separately, Cer 2 (a), Cer IIIa (b) or cutaneous lipids (LIP) (c) at constant concentrations. Mol were added at different increasing concentrations into the solution [lipid–DPH]. In the three models tested, only OC decreased significantly the fluorescence intensity. After a certain concentration, the fluorescence increased with Cer 2 and LIP. For Cer IIIa, the fluorescence remained low with the different OC concentrations tested.

We compared I_{fluo} variation between [OC] = 0 M and the threshold concentration for each lipidic model. For Cer 2 and Cer IIIa, I_{fluo} lost a maximum of 167 and 220 AUF respectively after the addition of a concentration of [OC] = 4×10^{-6} M into the [DPH–Lip] solution. For LIP, I_{fluo} lost a maximum of 82 AUF after the addition of 10^{-6} M of OC. After these threshold values reached, 4×10^{-6} M and 10^{-6} M respectively for Cer 2 and LIP, I_{fluo} increased. OC was able to induce a lipophilic environment after reaching the threshold concentration to interact with DPH and increased the fluorescence intensity in consequence with the Cer 2 and LIP. For Cer IIIa, the I_{fluo} did not vary significantly between 4×10^{-6} M and 2×10^{-5} M, I_{fluo} variation remained at the lowest value, showing that OC had a stronger interaction for the Cer IIIa rather than with the DPH. Moreover, OC showed the highest fluorescence variation with the Cer IIIa.

The lack of significant variation of I_{fluo} for the other molecules may be explained by their inability to "remove" the [probe–lipid] complex. It may have been caused in part by the DPH polarity (Log Pow = 5.6) compared to the polarity of the other molecules. The difference of Log Pow prevented the exogenous molecules, except OC that had the highest Log Pow (Log Pow = 6.88), to enter in competition with the DPH for interacting with the lipidic chains.

As DPH had the highest I_{fluo} in solution with Cer IIIa and highest I_{fluo} variation after addition of OC, this lipid was selected for the predictive approach protocol.

For the predictive approach, two UV filters with a Log Pow closer to DPH, octisalate (OS) (Log Pow = 5.77) and octinoxate (OX) (Log Pow = 5.8), were added to the study and more hydrophilic molecules removed (CAF, PRED, MP and EP). The molecule concentration was set at 10^{-5} M as at this concentration is high so molecules will in sufficient quantity to enter in competition with the DPH and at this concentration OC remained in interaction with the ceramides chains.

3.2. Predictive approach: determination of the Cer IIIa and Mol interaction criterion.

For the predictive approach, a new protocol was developed with a constant Cer IIIa and Mol concentration and a variation of DPH concentration. The concentration of Cer IIIa was set at 2×10^{-5} M and Mol concentration at 10^{-5} M. Increasing concentration of DPH were tested from 10^{-9} M to 2×10^{-6} M. The DPH concentration variation was based on a protocol initiated in a previous study with phospholipids (Caudron et al., 2007).

The fluorescence intensity of [DPH–Cer IIIa] solution was represented as I_{fluo} (MolFree) without molecules and as I_{fluo} (Mol) with Mol into the solution. We observed 3 different curves profiles (Fig. 4):

$$I_{fluo}(\text{Mol}) = I_{fluo}(\text{MolFree}) \quad \text{(A)}$$

For BP3 and BP, the I_{fluo} (MolFree) and I_{fluo} (Mol) were not notably different. There was no competition between BP3, BP and DPH for the Cer IIIa. No specific interactions were detected for these two molecules with the Cer IIIa. This observation showed the unability of the model to highlight specific interaction between molecule and Cer IIIa when the molecules polarity are quite lower than the probe polarity:

$$I_{fluo}(\text{Mol}) < I_{fluo}(\text{MolFree}) \quad \text{(B)}$$

For OX and OC, the I_{fluo} (Mol) was lower than I_{fluo} (MolFree). This observation highlights that an interaction between these molecules and Cer IIIa occured. I_{fluo}(OC) stayed closed to zero overall the DPH concentration range and showed a stronger interaction [OC–Cer IIIa] than [OX–Cer IIIa]. OC interacted with Cer IIIa and not with the probe. I_{fluo}(OX) was close to zero until the addition of a DPH concentration of 8×10^{-8} M, after this threshold I_{fluo}(OX) increased to reach the same intensity as I_{fluo} (MolFree) for the highest concentration. The I_{fluo} increase may be due to OX removal from the lipidic chain and to its interaction with DPH. OC had a stronger interaction with Cer IIIa compared to OX:

$$I_{fluo}(\text{Mol}) > I_{fluo}(\text{MolFree}) \quad \text{(C)}$$

I_{fluo} (OS) was higher than I_{fluo} (MolFree) after the addition of 7×10^{-8} M of OS. The complex [OS–DPH] fluoresced more than the complex [Cer–DPH]. OS may have had more affinity for the DPH than for the Cer IIIa. OS was able to induce a lipophilic environment for the DPH to fluoresce complexed to OS.

From these results, we proposed a fluorescence criterion to evaluate Mol–Cer interaction as a model to highlight a potential interaction between Mol and the SC lipids. The fluorescence criterion (ΔI) was the difference of fluorescence intensity at [DPH] = 10^{-7} M between I_{fluo} (MolFree) and I_{fluo} (Mol): the 10^{-7} M DPH concentration was chosen as this concentration was within the dynamic zone of response:

$$\Delta I = I_{fluo}(\text{MolFree}) - I_{fluo}(\text{Mol})$$

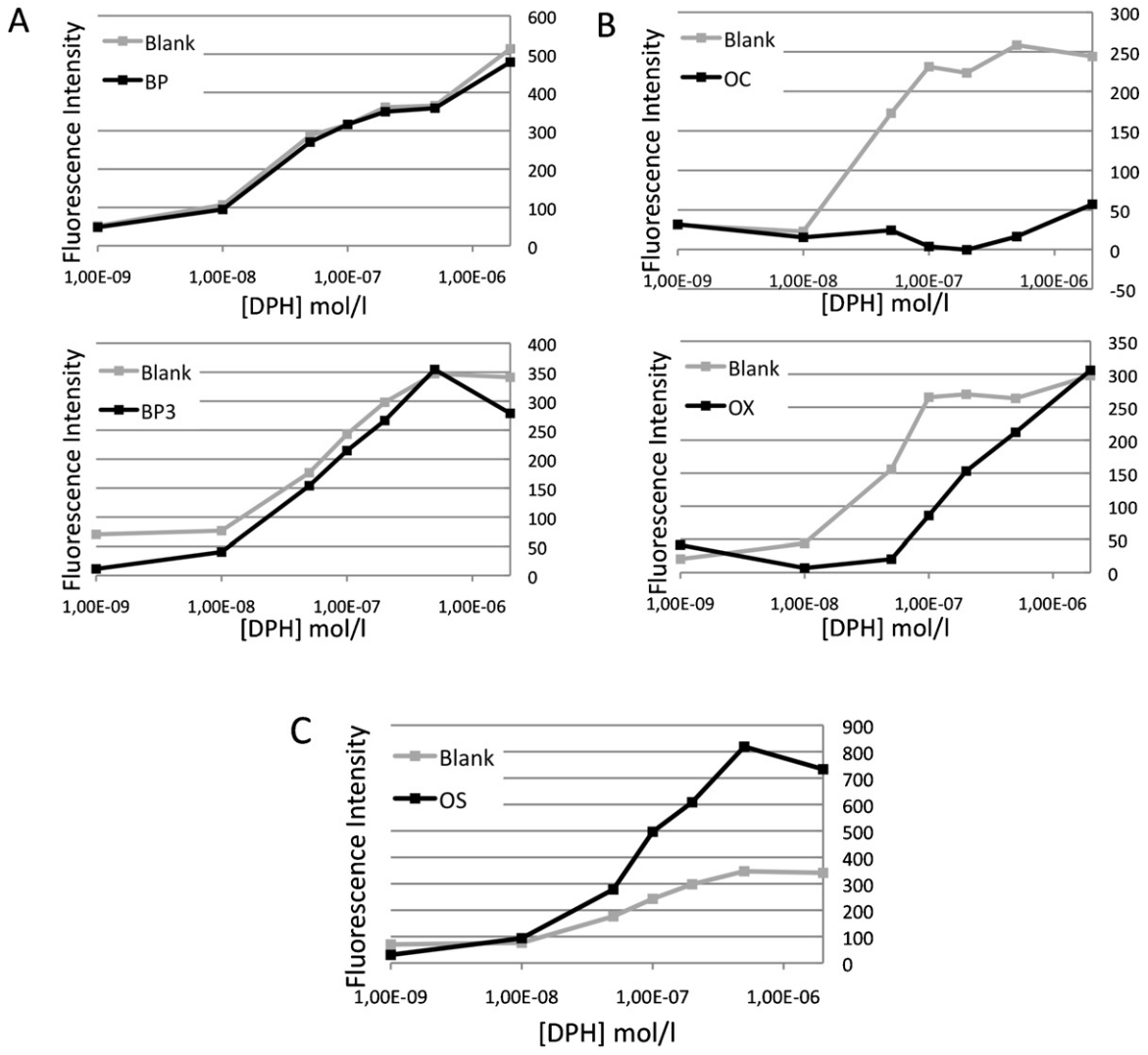

Fig. 4. Variation of fluorescence intensity in the predictive approach with a variation of DPH concentration and a constant exogenous molecules (Mol) and Cer IIIa concentrations. Mol were butyl paraben (BP), benzophenone 3 (BP3), octinoxate (OX), octisalate (OS) and octocrylene (OC). Each Mol was added separately to the [DPH–Cer IIIa] solution and the variation of fluorescence intensity variation was recorded after 10 min. Three profiles were observed A–C. The white curve represents the fluorescence curve with [Cer IIIa–DPH], I_{fluo} (MolFree), and the black the fluorescence curve with Mol added to [Cer IIIa–DPH], I_{fluo} (Mol).

Mol were classified in function of their interaction with the Cer IIIa, represented by the fluorescence criterion, ΔI that showed their potential interaction with SC ceramides (Table 3). $\Delta I = 0$ meant no interaction between Mol and Cer IIIa occured, $\Delta I > 0$ meant that Mol interacted with Cer IIIa and $\Delta I < 0$ meant that Mol interacted more with DPH than with the Cer IIIa.

3.3. Percutaneous penetration results

The molecules of interest were detected in each compartment 22 h after the deposit except in the liquid receptor. The average amount ($n = 3$) of molecules quantity distribution within tape stripping, epidermis, dermis and liquid receptor was summarized in Table 4. The ratio EP_{tot}/DE was calculated in order to show the proportion of molecule present in the total epidermis compared to the quantity detected in the dermis. The higher was the ratio EP_{tot}/DE, the more the molecule was retained in the total epidermis compared to the dermis.

Table 3
Exogenous molecules ranged in function of their fluorescence criterion ΔI.

	ΔI	Log Pow	MW
OS	−253.8	5.77	250
BP	0	3.53	194
BP3	28.25	3.79	228
OX	179.24	5.8	290
OC	227.41	6.88	351

BP ($EP_{tot}/DE = 6.9$) and BP3 ($EP_{tot}/DE = 6.4$) had the lower Log Pow and EP_{tot}/DE ratio within the five tested molecules. They tended to be more present in the dermis rather than the epidermis compared to the other molecules tested. OC ($EP_{tot}/DE = 10.0$) and OX ($EP_{tot}/DE = 15.1$) were proportionally the most retained n the epidermis. OX that had the same polarity as OS ($EP_{tot}/DE = 8.3$) was proportionally much more distributed into the epidermis than the dermis. OC that was the most apolar molecule had a smaller ratio at 10.0 compared to OX meaning that OC was less retained in the epidermis than OX. The ratio value (EPtot/DE) of these three molecules (OC, OX and OS) was not completely related to their Log Pow or MW.

3.4. Comparison of the percutaneous penetration results with the fluorescence criterion and Log Pow

The fluorescence intensity curves in comparison of the molecules distribution profile provided relevant information. For

Table 4
Molecule quantity (nmol/cm^2) within the 3 tapes stripping (TS), epidermis (EP), total epidermis (EPtot = TS + EP), dermis (DE) and the ratio EP_{tot}/DE.

	TS	EP	DE	LR	EP_{tot}	EP_{tot}/DE
BP	250.0 ± 106.0	88.1 ± 37.6	49.6 ± 5.4	≤LOD	338.1	6.8
BP3	161.5 ± 12.7	131.9 ± 31.3	54.1 ± 22.1	≤LOD	293.3	5.4
OS	187.9 ± 30.2	107.7 ± 19.8	35.4 ± 10.3	≤LOD	295.6	8.3
OX	173.3 ± 29.9	150.1 ± 65.6	21.4 ± 7.8	≤LOD	323.3	15.1
OC	186.5 ± 73.5	142.4 ± 15.2	32.8 ± 11.5	≤LOD	329.0	10

example, BP3 and BP had the same fluorescence curve profile, they did not enter in competition with the DPH for the Cer IIIa and they had the lower EP_{tot}/DE ratio. These observations meant that BP and BP3 were proportionally less retained in the epidermis and had no specific interaction with the SC lipids compared to the other molecules. The fluorescence criterion revealed that OC and OX had affinity for the Cer IIIa and their distribution showed that these molecules were proportionally more retained in the epidermis compared to the dermis. Despite their different Log Pow, OX and OC seemed to have similar interaction with SC lipids within the epidermis. OS that have the same polarity as OX, had a different affinity for the ceramide in fluorescence and was proportionally much less retained in the epidermis compared to OX. ΔI was more related to the distribution profile of the molecules within the skin.

To confirm these observations a correlation was performed between the fluorescence criterion ΔI and the Log Pow of the molecules tested. The results are illustrated in Fig. 5. It was difficult to correlate ΔI (OS) ($\Delta I < 0$) with the other ΔI ($\Delta I > 0$) ΔI had opposite value. In consequences, correlations were calculated with and without OS. ΔI and Log Pow were very much correlated ($R^2 = 0.99$) without OS but not correlated at all with OS ($R^2 = 0.08$). This correlation indicates that polarity seems to be very representative of the ceramide and exogenous molecule interaction in this study, meaning that this interaction may be mainly due to the lipophily. For most of the molecules, Log Pow was sufficient to predict their skin distribution profile, but if the molecule did not enter into the correlation, such as OS, it means that this molecule had a lower retention that was represented by its fluorescence criterion ΔI.

In parallel we expressed our results according to the SCCS recommendations (SCCS, 2010). The SCCS claims that both the epidermis (except for the stratum corneum) and dermis are considered as a sink. The amounts found in these compartments are considered as absorbable and are added to those found in the receptor fluid. The amounts that are retained by the stratum corneum at the time of sampling are not considered to be dermally absorbed, and thus they are not expected to contribute to the systemic dose. We expressed the epidermal and dermal absorption (EP + DE) in absolute amount of skin surface (μg/cm^2) in Table 5. We did not consider the amount in the LR as the quantity detected was less than the limit of detection. There might be SC left in EP as the 3 tapes stripping on human biopsies did not remove the entire SC. We expressed EP + DE molecule quantity detected in function of the ΔI and Log Pow (Fig. 6). A strong correlation was not observed neither

Table 5
Molecule quantity (μg/cm^2) within the 3 tapes stripping (TS), epidermis (EP), dermis (DE) and EP + DE.

	TS	EP	DE	LR	EP + DE
BP	48.5 ± 20.6	17.1 ± 7.3	49.6 ± 1.0	≤LOD	26.7
BP3	36.8 ± 2.9	30.1 ± 7.1	54.1 ± 5.0	≤LOD	42.4
OS	47.0 ± 8	26.9 ± 5	35.4 ± 3	≤LOD	35.8
OX	54.5 ± 8.7	31.2 ± 19.0	21.4 ± 2.3	≤LOD	41.5
OC	65.5 ± 25.8	50.0 ± 5.3	32.8 ± 4.0	≤LOD	61.5

for Log Pow nor ΔI with EP + DE ($R^2 = 0.53$ and 0.38 respectively). The four molecules, BP, BP3, OX and OC epidermal and dermal distribution were quite related to the ΔI and Log Pow ($R^2 = 0.67$ and 0.71 respectively). However, Log Pow did not highlight the particular behavior of OS, this was only possible with the fluorescence criterion ($\Delta I < 0$).

The ratio EP_{tot}/DE seems more relevant than EP + DE in this work to compare the fluorescence criterion calculated with the Franz cells data. The ratio calculated reflected here the fast kinetic of OS at 22 h. This observation was not possible to determine with EP + DE.

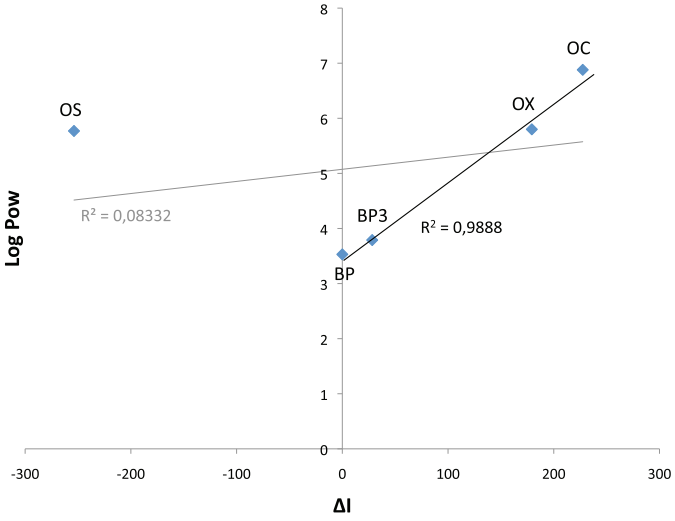

Fig. 5. Correlation between exogenous molecules fluorescence criterion (ΔI) and their polarity (Log Pow). The correlation was calculated with OS ($R^2 = 0.08332$) and without OS ($R^2 = 0.9888$).

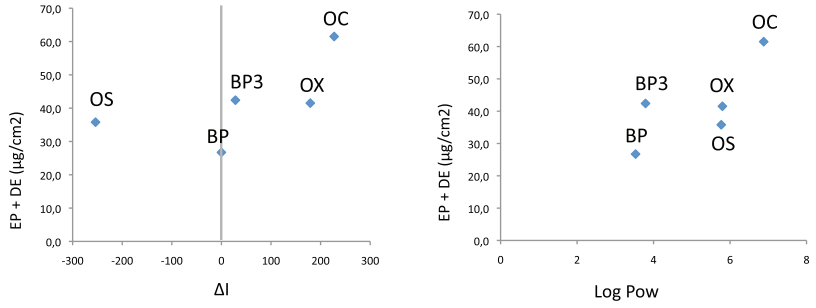

Fig. 6. Epidermal and dermal quantity (μg/cm^2) expressed in function of the fluorescence criterion (ΔI) and Log Pow.

4. Conclusion

Our study helped to understand the exogenous molecule and ceramide specific interaction with a fluorimetric indicator. Exogenous molecules were able to displace the [probe–lipid] equilibrium and this capacity was correlated to our percutaneous penetration data. Molecules with affinity for the Cer IIIa (OC and OX) were found to be proportionally more distributed into the epidermis. Molecules that were not able to remove the probe from the lipid (BP and BP3) were found to be the less proportionally distributed into the epidermis. These results revealed that the nature of the ceramide and exogenous molecules interaction is mainly of a lipophilic nature but the fluorescence criterion defined provided complementary information. The fluorescence criterion (ΔI) highlighted the particular interaction of some molecules with the ceramide and their skin distribution. This particular behavior was not initially possible to estimate with the Log Pow and MW. It was not possible to test molecules with a too high difference of polarity with the probe: molecules with a much lower Log Pow were not able to enter in competition with the probe. The protocol of the predictive approach can now be transposed to more investigations with other fluorescence probes and cutaneous lipids.

This study showed the interest of a new criterion, a fluorescence criterion, which characterized the interaction between cutaneous ceramides and exogenous molecules. Because of the limitation of ex vivo protocols by Franz cells for the study of percutaneous penetration and their lack of homogeneity, there is a real need to improve predictive models with a constant protocol for the risk analysis of new compounds. This new criterion could help to develop more improved mathematical models in complement of the current coefficient used.

Acknowledgements

We acknowledge Dr Ionnis Nicolis for his help with the interpretation, Dr Eric Caudron for his help with the fluorescence protocole, Wen Fang, Naira Perez and Yuan Gao for their help with the experiments.

References

Benson, H.A.E., Watkinson, A.C., 2011. Topical and Transdermal Drug Delivery: Principles and Practice. John Wiley & Sons, New Jersey.

Caudron, E., Zhou, J.Y., Chaminade, P., Baillet, A., Prognon, P., 2005. Fluorescence probe assisted post-column detection for lipid analysis in microbore-LC. J. Chromatogr. A 1072, 149–157.

Caudron, E., Zhou, J.Y., England, P., Ollivon, M., Prognon, P., 2007. Some insights about 1,6-diphenyl-1,3,5-hexatriene-lipid supramolecular assemblies by steady-state fluorescence measurements. Appl. Spectrosc. 61, 963–969.

Ghafourian, T., Samaras, E.G., Brooks, J.D., Riviere, J.E., 2010. Validated models for predicting skin penetration from different vehicles. Eur. J. Pharm. Sci. 41, 612–616.

Grégoire, S., Ribaud, C., Benech, F., Meunier, J.R., Garrigues-Mazert, A., Guy, R.H., 2009. Prediction of chemical absorption into and through the skin from cosmetic and dermatological formulations. Br. J. Dermatol. 160, 80–91.

Guy, R.H., Potts, R.O., 1992. Predicting skin permeability. Pharm. Res. 9, 663–669.

Ibrahim, H., Kasselouri, A., Raynal, B., Pansu, R., Prognon, P., 2011. Investigating the possible use of a tetra (hydroxyphenyl) porphyrin as a fluorescence probe for the supramolecular detection of phospholipids. J. Lumin. 131, 2528–2537.

Janssens, M., van Smeden, J., Gooris, G.S., Bras, W., Portale, G., Caspers, P.J., Vreeken, R.J., Kezic, S., Lavrijsen, A.P., Bouwstra, J.A., 2011. Lamellar lipid organization and ceramide composition in the stratum corneum of patients with atopic eczema. J. Invest. Dermatol. 131, 2136–2138.

Janůšová, B., Zbytovská, J., Lorenc, P., Vavrysová, H., Palát, K., Hrabálek, A., Vávrová, K., 2011. Effect of ceramide acyl chain length on skin permeability and thermotropic phase behavior of model stratum corneum lipid membranes. Biochim. Biophys. Acta 1811, 129–137.

Joo, K.M., Nam, G.W., Park, S.Y., Han, J.Y., Jeong, H.J., Lee, S.Y., Kim, H.K., Lim, K.M., 2010. Relationship between cutaneous barrier function and ceramide species in human stratum corneum. J. Dermatol. Sci. 60, 47–50.

Kessner, D., Ruettinger, A., Kiselev, M.A., Wartewig, S., Neubert, R.H., 2008. Properties of ceramides and their impact on the stratum corneum structure. Part 2. Stratum corneum lipid model systems. Skin Pharmacol. Physiol. 21, 58–74.

Lian, G., Chen, L., Han, L., 2008. An evaluation of mathematical models for predicting skin permeability. J. Pharm. Sci. 97, 584–598.

Masukawa, Y., Narita, H., Shimizu, E., Kondo, N., Sugai, Y., Oba, T., Homma, R., Ishikawa, J., Takagi, Y., Kitahara, T., Takema, Y., Kita, K., 2008. Characterization of overall ceramide species in human stratum corneum. J. Lipid Res. 49, 1466–1476.

Novotný, J., Janůsová, B., Novotný, M., Hrabálek, A., Vávrová, K., 2009. Short-chain ceramides decrease skin barrier properties. Skin Pharmacol. Physiol. 22, 22–30.

Organization for Economic Co-operation and Development (OECD), 2010. Guidance Document for the Conduct of Skin Absorption Studies, www.oecd.org/dataoecd/0/1/46257610.pdf (accessed 25.03.12).

Organization for Economic Co-operation and Development (OECD), 2008. OECD Guideline for the Testing of Chemicals, www.oecdbookshop.org/oecd/display.asp?sf1=identifiers&st1=9789264071087 (accessed 07.05.12).

Scientific Committee on Consumer Safety (SCCS), SCCS/1358/10, 2010 Basic Criteria for the In Vitro Assessment of Dermal Absorption of Cosmetic Ingredients.

Wartewig, S., Neubert, R.H., 2007. Properties of ceramides and their impact on the stratum corneum structure: a review. Part 1. Ceramides. Skin Pharmacol. Physiol. 20, 220–229.

Zhou, J.Y., Chaminade, P., Gaudin, K., Prognon, P., Baillet, A., Ferrier, D., 1999. Postcolumn fluorescence as an alternative to evaporative light scattering detection for ceramide analysis with gradient elution in non-aqueous reversed-phase liquid chromatography. J. Chromatogr. A 859, 99–105.